

A Possible Rossby Wave Instability Origin for the Flares in Sagittarius A*

Michel Tagger

*Service d'Astrophysique, (UMR AstroParticules et Cosmologie), CEA Saclay
91191 Gif-sur-Yvette, France
tagger@cea.fr*

Fulvio Melia¹

*Departments of Physics and Astronomy, The University of Arizona,
Tucson AZ 85721, USA
fmelia@as.arizona.edu*

ABSTRACT

In recent years, near-IR and X-ray flares have been detected from the Galaxy's central radio point source, Sagittarius A* (Sgr A*), believed to be a $\sim 3 \times 10^6 M_\odot$ supermassive black hole. In some cases, the transient emission appears to be modulated with a (quasi-)periodic oscillation (QPO) of $\sim 17 - 20$ minutes. The implied $\sim 3 r_S$ size of the emitter (where $r_S \equiv 2GM/c^2$ is the Schwarzschild radius) points to an instability—possibly induced by accretion—near the Marginally Stable Orbit (MSO) of a slowly spinning object. But Sgr A* is not accreting via a large, ‘standard’ disk; instead, the low density environment surrounding it apparently feeds the black hole with low angular momentum clumps of plasma that circularize within $\sim 10 - 300 r_S$ and merge onto a compact, hot disk. In this *Letter*, we follow the evolution of the disk following such an event, and show that a Rossby wave instability, particularly in its magnetohydrodynamic (MHD) form, grows rapidly and produces a period of enhanced accretion lasting several hours. Both the amplitude of this response, and its duration, match the observed flare characteristics rather well.

Subject headings: accretion—black hole physics—Galaxy: center—magnetohydrodynamics—plasmas—Instabilities

1. Introduction

The prospect of identifying phenomena within several Schwarzschild radii ($r_S \equiv 2GM/c^2$) of Sgr A* has improved considerably in recent years, with the detection of near-IR (Genzel et al. 2003) and X-ray (Bélanger et al. 2005) flares modulated with an average period of $\approx 17 - 20$ minutes (Bélanger et al. 2006). This (quasi-)period corresponds to a modulation near the MSO of the black hole (Melia et al. 2001; Liu & Melia 2002), possibly suggesting a transient event associated with a wave pat-

tern co-rotating with the gas, or perhaps a “hot” spot where matter has fallen in from larger radii, impacting the small disk (Falcke & Melia 1997). In this *Letter*, we examine numerically the Rossby wave instability (RWI) induced by a clump of magnetized plasma merging onto the disk and focus on its implications for the subsequent flow of matter through the MSO toward the event horizon.

For a black hole mass $M \sim 3 \times 10^6 M_\odot$, the radius $r \approx 3 r_S$ inferred from the average period is interesting for several reasons. Aside from constraining the flaring event to a region very near the MSO, it supports the view that there is indeed a

¹Sir Thomas Lyle Fellow and Miegunyah Fellow.

hot, magnetized disk confined to the inner $\sim 10r_S$ that can simultaneously produce a $\approx 10\%$ polarized component and a position angle that rotates by 90° across the mm/sub-mm bump (Bromley, Melia, & Liu 2001). In addition, strong variability is seen near the middle of these events, in which the X-ray flux drops by a factor of 40–50 % in 10–15 minutes. Simple light travel time arguments constrain the emitting region to be no bigger than $\sim 17 - 34 r_S$ (Melia 2001). This tight orbit suggests that the X-ray and mm/sub-mm photons are produced by the same medium, probably via synchrotron-self-Compton processes. Finally, this is in line with the measured intrinsic size of Sgr A* at $\lambda 7$ mm (Bower et al. 2004).

Extensive hydrodynamic (Melia & Coker 1999; Cuadra et al. 2005) and MHD (Igumenshchev & Narayan 2002) simulations show that for the stellar-wind fed conditions at the Galactic center, the average specific angular momentum of gas captured gravitationally by Sgr A* is too small to sustain a ‘conventional’ (i.e., typically large $\sim 10^5 r_S$) disk. Instead, only clumps of plasma with relatively small angular momentum venture inwards and merge with—essentially, ‘rain’ onto—the compact disk at the circularization radius, which for Sgr A* is $\lesssim 10 - 10^3 r_S$ (see also Melia & Falcke 2001, Melia 2006). In this paper, we model the transient disruption to the disk induced by blobs of plasma circularizing within the inner $\sim 10 - 20 r_S$, and show that the ensuing dynamical evolution has characteristics in common with those inferred from the flares.

2. Magnetic Rossby Wave Instability

The instability we are here concerned with has a long history, dating back to Lovelace & Hohlfeld (1978), who showed that a disk presenting an extremum of a quantity \mathcal{L} (later dubbed vortensity) was subject to a local instability of Rossby vortices. The requirement of an extremum is similar to that giving rise to the Kelvin-Helmholtz instability of sheared flows. More recently, Lovelace et al. (1999) (see also Li et al. 2000, Li et al. 2001) renamed it the Rossby Wave Instability (RWI) and developed the theory and numerical simulation. Varnière & Tagger (2005) used it to address the presence of a ‘Dead Zone’ in protostellar disks.

In isothermal, unmagnetized disks, \mathcal{L} is the spe-

cific vorticity averaged across the disk thickness,

$$\mathcal{L} = \frac{\vec{\nabla} \times \vec{V}}{\Sigma} = \frac{\kappa^2}{2\Omega\Sigma}, \quad (1)$$

where Σ is the disk’s surface density, Ω its rotation frequency, and $\kappa^2 = 4\Omega^2 + 2\Omega\Omega'r$ is the epicyclic frequency squared. The extremum of \mathcal{L} appears to be due to an extremum in the radial density profile. However, starting from a very different point of view—the seismology of relativistic accretion disks—Nowak & Wagoner (1991) described g-modes that introduce an extremum in κ , and thus also in \mathcal{L} (though this time due to the relativistic rotation curve), near the MSO (where κ vanishes). The g-mode of Nowak & Wagoner is thus similar to the RWI, but they seem to have missed the mechanism that makes it unstable. Its tentative association with a QPO in X-ray binaries does not seem to be supported by observations. We will see, however, that it plays an important role in what follows.

Many of the details regarding how the instability is driven have already appeared in the work cited above. The main idea is that Rossby waves in disks form normal modes trapped near the extremum of \mathcal{L} . The waves propagate either outside or inside their corotation radius, i.e., the radius where the wave rotates at the same frequency as the gas, depending on the sign of the gradient in \mathcal{L} (Tagger 2001). They have a positive energy in the first case, and a negative energy in the second. In a forthcoming paper, we shall discuss the MHD form of the RWI, for a disk threaded by a vertical (poloidal) magnetic field $B_0(r)$. Its properties are essentially the same as those discussed above, except that here the critical quantity is $\mathcal{L}_B = \kappa^2\Sigma/(2\Omega B_0^2)$, and the growth rate can be higher because of the long-range action of the Lorentz force coupling the Rossby vortices (Tagger & Pellat 1999). Another difference is that the energy and angular momentum of the Rossby waves can escape the disk vertically as Alfvén waves propagating along the magnetic field lines (Varnière & Tagger 2002).

Let us finally mention that even without an extremum in \mathcal{L} or \mathcal{L}_B , normal modes may still occur if the disk has an inner edge that reflects spiral density waves. In magnetized disks this gives the Accretion-Ejection Instability (Tagger & Pellat 1999). Recently, Li et al. (2003) dis-

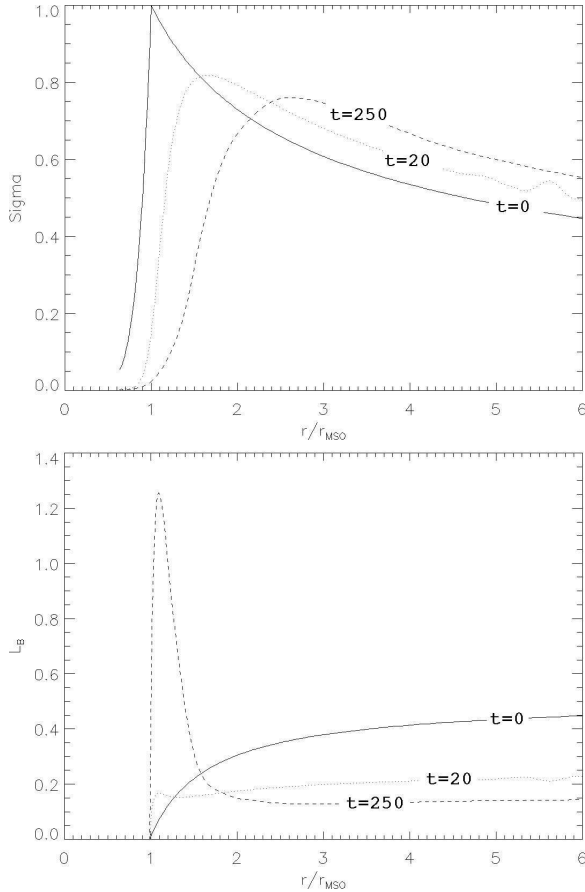


Fig. 1.— Surface density (top) and \mathcal{L}_B (bottom) profiles, at startup (full) and after 20 (dashed) and 250 (dot-dashed) M_{SO} orbital times in our first simulation. Radii are scaled to r_{MSO} .

cussed the non-axisymmetric g-modes and concluded that those without nodes in their vertical structure (that we analyze here) are not unstable. But this conclusion, based on the absence of a reflecting inner edge in a relativistic disk, neglected the possibility of trapped modes based on Rossby, rather than density, waves.

3. Numerical simulations

The simulations presented here are relevant to the conditions in Sgr A*. We use the 2-D MHD code introduced in Caunt & Tagger (2001), that considers an infinitely thin disk in vacuum. This is well adapted to the physics we consider, since the RWI and spiral modes have a structure that is essentially constant across the disk thickness,

allowing us to integrate the dynamical equations over z . (On the other hand, this simplification forbids us to study the Magneto-Rotational Instability (MRI), whose structure does vary with z .)

The radial grid points are distributed logarithmically, allowing simulations that extend far in radius (typically with $r_{max}/r_{min} \approx 50$), so as to minimize unwanted boundary effects. We have modified the code by including the pseudo-Newtonian potential of Paczynski-Witta, $\Phi(r) = GM/(r - r_S)$. This allows for the existence of an MSO, $r_{MSO} = 3r_S$, where κ vanishes. Furthermore, at the inner grid point the gas is allowed to cross freely during its final collapse toward the central object. The simulations are carried out on a polar grid with $n_r = 256$ and $n_\theta = 128$ points, and extend from ~ 0.6 to $30 r_{MSO}$. The MSO is at the 30th radial grid point, allowing us to resolve properly the gas flow (including the sonic point) in the plunging region; the infall velocity at the inner boundary is typically 3 to 5 times the sound velocity. Since pressure does not play a major role in the physics of Rossby waves, we fix the sound speed as a function of radius, which for simplicity is kept constant throughout the simulations. We first present the simulation of a disk with initially a power-law surface density profile, $\Sigma \sim r^{-1/2}$, and a sound speed $c_S = .05 r\Omega(r)$, (giving a constant disk aspect ratio h/r). The initial magnetic field is such that $\beta \equiv 8\pi p/B^2 = 2$ throughout the disk. After a few orbits, the density profile near the MSO reaches a quasi-steady state, as shown in Figure 1 (here and below we scale all radii to r_{MSO} and times to the orbital period there). This is very similar to what is obtained with 3-D codes (Hawley & Krolik 2001; Machida & Matsumoto 2003). An $m=1$ perturbation, identified as a g-mode instability by the RWI mechanism, sets in, gradually eroding the inner edge of the disk (since there is no turbulent accretion from farther out). This builds up the extremum of \mathcal{L}_B just beyond the MSO. The instability has its corotation radius near the extremum, as expected. The accretion rate \dot{M} through the disk peaks when the instability gets established, and then decreases gradually for the rest of the simulation, as the density maximum slowly moves outward.

In our second calculation, we simulate a flare event by adding to the ‘standard’ disk a strong bump in density and magnetic field centered at

$4 r_{MSO}$, where it generates a minimum in \mathcal{L}_B . This bump represents 56% of the total mass in the central $6 r_{MSO}$. Pursuant to our discussion in the introduction, we assume that a blob of magnetized plasma with very little angular momentum has merged onto the disk, rapidly circularizing to form a ring at this radius. As shown in Figure 2, the evolution is much more violent. In a nearly sudden episode between 40 and 60 MSO orbital times (hardly 2 periods at $4r_{MSO}$, or in real time about 5 hours), most of the added gas has been transported to the inner region of the disk by violent instabilities developing over the whole region.

We see $m = 1$ modes developing (as previously) near the inner edge, and $m = 2$ in the bump region, with a corotation near the extremum of \mathcal{L}_B . These modes appear to be non-linearly coupled; similar coupling has been observed in simulations and observations of spiral galaxies (Tagger et al. 1987; Masset & Tagger 1997). This coupling can be explosive (i.e., result in faster than exponential growth) when it involves modes of positive and negative energy (Dikasov et al. 1969). Figure 3 shows the surface density profile at $t = 40t_{MSO}$, when the density bump starts being disrupted by the instability. Figure 2 shows that after this rapid phase, the radial profile of \mathcal{L}_B becomes perfectly flat beyond the MSO region, confirming qualitatively that it is that profile to which the instability reacts.

Producing realistic light curves involves much more physics than we include here, and is beyond the scope of the present simulations. However, figure 4 shows \dot{M} through the inner edge of the simulation box. Notice the brief episode of strong, enhanced accretion between $t = 40t_{MSO}$ and $t = 60t_{MSO}$, with the largest amplitude occurring over a time interval of roughly $7t_{MSO}$ (i.e., ~ 140 minutes). The similarity between this time and the duration of a typical flare ($\sim 2-3$ hours) is very encouraging. Also, there is clear evidence of 4 or 5 quasi-periodic pulsations during this phase of enhanced accretion, mimicking the behavior witnessed during several IR flares and the XMM event of 2004. This appears to be due to an axisymmetric g-mode, trapped near the extremum of \mathcal{L}_B and non-linearly excited by the instabilities. The details may vary with the numerical setup, e.g., with the amount of artificial viscosity; this is rea-

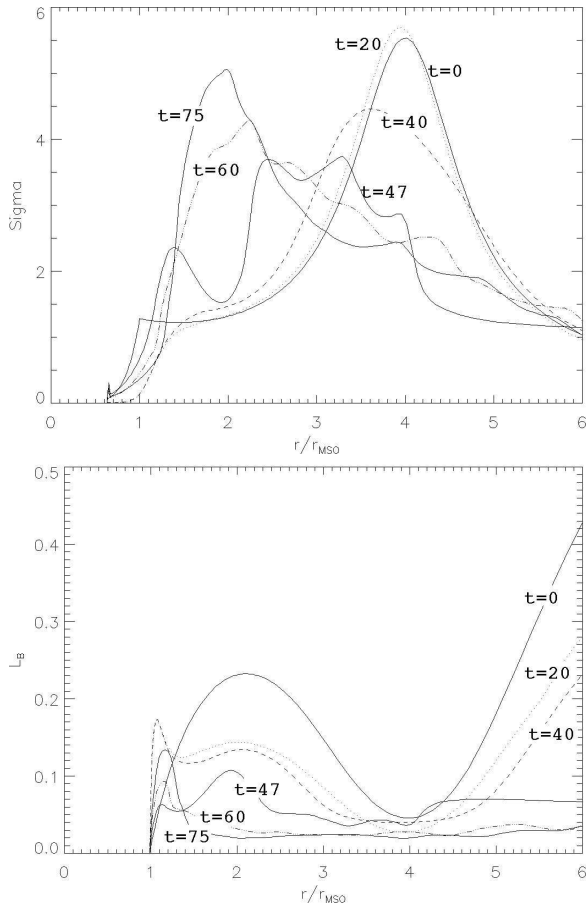


Fig. 2.— Surface density (top) and \mathcal{L}_B (bottom) profiles, at startup (full) and after 20 , 40, 47, 60, 75 MSO orbital times during our second simulation.

sonable since this is the only dissipation limiting the growth of the instability in the simulations (besides the destruction of the bump itself), but the main features (duration of the flare and pulsations) remain the same.

Simulations of less magnetized or unmagnetized disks, or of a weaker bump, give a very similar, though somewhat slower, evolution. Placing the bump at 6 or $8 r_{MSO}$ delays the development of the instability, but does not change the duration or the amplitude of the ‘flare’, which occurs only when the mass of the accreted gas approaches the MSO. However this might result in changes of the mm and cm emissivity relative to the IR/X-ray emission, so a comparative study of the broadband spectrum of many flares may provide indirect ev-

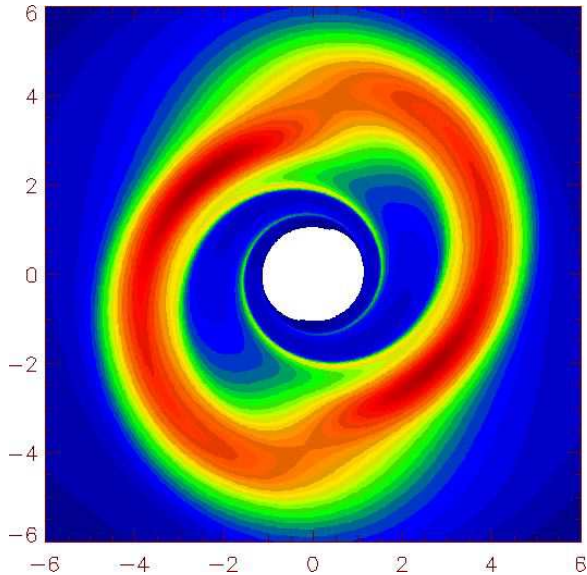


Fig. 3.— Surface density in our second simulation at $t = 40 t_{MSO}$, when the bump at $4 r_{MSO}$ (red, dark) starts being disrupted by the instability.

idence of the variation in clumping radius.

4. Conclusion

The RWI, particularly in its MHD form, can produce the behavior required to account for the near-IR and X-ray flares in Sgr A*. Unstable both near the MSO and in the annulus where a clump of interstellar plasma has merged onto the disk, it develops as strong Rossby vortices whose non-linear evolution can be remarkably fast. The instability grows in a few rotation times, and causes the clump to accrete to the inner edge of the disk. The resulting period of enhanced \dot{M} at the inner edge corresponds to the final stage of this collapse, so that its duration (comparable with the observed duration of the flares) does not depend on the initial location of the clump. Furthermore, the enhanced \dot{M} is accompanied by QPO very similar to those observed both in IR and in X-rays. The quasi-period reflects the underlying Keplerian frequency near the MSO, though the exact quasi-period may be dependent on our use of a pseudo-Newtonian potential, rather than a fully relativistic model. Natural extensions will thus be to include the metric of a spinning Black Hole, and to consider the relevance of the RWI to explain the high-frequency QPO in microquasars.

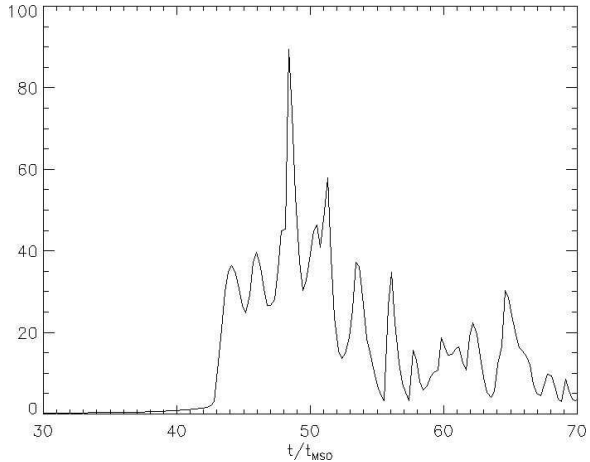


Fig. 4.— Accretion rate through the inner edge of the simulation box in the second simulation.

While current wisdom seems to be settling on an accretion instability for the origin of Sgr A*'s flares, the process by which the actual emission occurs is uncertain. The favored scenario right now connecting the mm/sub-mm to NIR and X-rays portions of the spectrum (Eisenhauer et al. 2005; Liu & Melia 2001) is that the former is due to synchrotron, whereas the X-rays are produced by synchrotron-self-Compton (SSC). It turns out that producing the right blend of physical conditions to fit both the NIR and X-ray flare emission (under the assumption that the two occur more or less simultaneously) is not trivial.

In a related paper (Liu, Melia & Petrosian 2005), we considered a scenario in which the radiative manifestation of the flare occurs when the energy released by the accretion instability is transferred to a population of nonthermal particles via stochastic acceleration by the turbulent component of the magnetic field. Indeed, as mentioned in §2, Rossby waves in the disk extend into the corona as Alfvén waves, carrying much of the accretion energy. Clearly, much work remains to be done in coupling these complementary approaches. One of the main results reported in this paper is that the enhanced \dot{M} during a flare event is consistent—both in amplitude and temporal evolution—with the characteristics observed in Sgr A*'s flares. We are in the process of self-consistently calculating the particle acceleration following an RWI-induced event, and will report the results of this work in a future publication.

This research was partially supported by NSF grant AST-0402502 (at Arizona). FM is grateful to the College de France, where this work was carried out. MT wishes to thank P. Varnière for help with the numerical simulations. FM and MT thank G. Bélanger for stimulating discussions.

REFERENCES

- Bélanger, G., Goldwurm, A., Melia, F. et al. 2005, ApJ, in press
- Bélanger, G., Goldwurm, A., Melia, F. et al. 2006, ApJ, submitted
- Bower, G. C., et al. 2004, Science, 304, 704
- Bromley, B., Melia, F., & Liu, S. 2001, ApJ, 555, L83
- Caunt, S. E., & Tagger, M. 2001, A&A, 367, 1095
- Cuadra, J., Nayakshin, S., Springel, V., & Di Matteo, T. 2005, MNRAS, 360, L55
- Dikasov, V., Rudakov, L., & Ryutov, D. . 1969, Sov. Phys. JETP, 17, 403
- Drazin, P. G., & Reid, W. H. 2004, Hydrodynamic Stability. ISBN 0521525411. Cambridge, UK: Cambridge University Press, September 2004.
- Eisenhauer, F. et al. 2005, ApJ, submitted
- Falcke, H. & Melia, F. 1997, ApJ, 479, 740
- Genzel, R. et al. 2003, Nature, 425, 934
- Hawley, J. F., & Krolik, J. H. 2001, ApJ, 548, 348
- Hollywood, J. M. & Melia, F. 1997, ApJS, 112, 423
- Hollywood, J. M., Melia, F., Close, L. M., et al. 1995, ApJ, 448, L21
- Igumenshchev, I.V. & Narayan, R. 2002, ApJ, 566, 137
- Krichbaum, T. P. et al. 2003, A&A, 335, L106
- Li, H., Colgate, S. A., Wendroff, B., & Liska, R. 2001, ApJ, 551, 874
- Li, H., Finn, J. M., Lovelace, R. V. E., & Colgate, S. A. 2000, ApJ, 533, 1023
- Li, L.-X., Goodman, J., & Narayan, R. 2003, ApJ, 593, 980
- Liu, S. & Melia, F. 2001, ApJ, 561, L77
- Liu, S. & Melia, F. 2002, ApJ, 566, L77
- Liu, S., Melia, F., & Petrosian V. 2005, ApJ, in press
- Lovelace, R. V. E., & Hohlfield, R. G. 1978, ApJ, 221, 51
- Lovelace, R. V. E., Li, H., Colgate, S. A., & Nelson, A. F. 1999, ApJ, 513, 805
- Machida, M., & Matsumoto, R. 2003, ApJ, 585, 429
- Mark, J. W.-K. 1976, ApJ, 203, 81
- Masset, F., & Tagger, M. 1997, A&A, 322, 442
- Melia, F. 2001, Nature, 413, 25
- Melia, F. 2006, in *The Galactic Supermassive Black Hole* (PUP: New York)
- Melia, F., Bromley, B., Liu, S., & Walker, C. 2001, ApJ, 554, L37
- Melia, F. & Coker, R.F. 1999, ApJ, 511, 750
- Melia, F. & Falcke, H. 2001, ARAA, 39, 309
- Narayan, R., Goldreich, P., & Goodman, J. 1987, MNRAS, 228, 1
- Nowak, M. A., & Wagoner, R. V. 1991, ApJ, 378, 656
- Papaloizou, J. C. B., & Pringle, J. E. 1985, MNRAS, 213, 799
- Tagger, M. 2001, A&A, 380, 750
- Tagger, M., & Pellat, R. 1999, A&A, 349, 1003
- Tagger, M., Sygnet, J. F., Athanassoula, E., & Pellat, R. 1987, ApJ, 318, L43
- Varnière, P., & Tagger, M. 2002, A&A, 394, 329
- . 2005, A&A, submitted

This 2-column preprint was prepared with the AAS L^AT_EX macros v5.2.